Visual Neuroscience

Microfluidics-Based Subretinal Chemical Neuromodulation of Photoreceptor Degenerated Retinas

Corey M. Rountree,[1] John B. Troy,[2] and Laxman Saggere[1]

[1]Department of Mechanical and Industrial Engineering, University of Illinois at Chicago, Chicago, Illinois, United States
[2]Department of Biomedical Engineering, Northwestern University, Evanston, Illinois, United States

Correspondence: Laxman Saggere, Department of Mechanical and Industrial Engineering, University of Illinois at Chicago, 842 W Taylor Street, Chicago, IL 60607, USA; saggere@uic.edu.

Submitted: October 11, 2017
Accepted: December 13, 2017

Citation: Rountree CM, Troy JB, Saggere L. Microfluidics-based subretinal chemical neuromodulation of photoreceptor degenerated retinas. *Invest Ophthalmol Vis Sci*. 2018;59:418–430. https://doi.org/10.1167/iovs.17-23142

Purpose. Retinal prostheses can restore rudimentary vision in cases of photoreceptor degeneration through electrical stimulation, but face difficulties achieving high spatial resolution because electrical current is an inherently unnatural stimulus. We investigated the therapeutic feasibility of using patterned delivery of the glutamate neurotransmitter, a primary agent of natural synaptic communication of the retina, as a biomimetic chemical alternative to electrical current for neuromodulation of photoreceptor degenerate retina.

Methods. We injected small quantities of the neurotransmitter glutamate into the subretina of 20 explanted photoreceptor degenerated S334ter-3 rat retinas using glass micropipettes and a prototype multiport microfluidic device to accomplish single- and multisite stimulation in vitro. The effects of chemical stimulation were characterized by recording neural responses from retinal ganglion cells (RGCs) using a multielectrode array.

Results. Subretinally injected exogenous glutamate activates RGCs, despite the substantial anatomic and physiologic changes caused by retinal remodeling, eliciting robust neural responses. The presence of excitatory and inhibitory RGC responses provides evidence that exogenous glutamate differentially activated neurons presynaptic to RGCs, likely inner retinal neurons belonging to the OFF and ON pathways. We also demonstrate that glutamate injections can evoke focal RGC responses with spatial resolutions comparable to or better than current generation electrical prostheses and, when applied at multiple sites simultaneously with the multiport microfluidic device, can produce spatially patterned neural responses.

Conclusions. These significant results establish that chemical stimulation of degenerated retinas with neurotransmitters is an effective neuromodulation strategy with the potential of restoring high-resolution visual perception in patients rendered blind through photoreceptor degeneration.

Keywords: photoreceptor degeneration, retina, chemical stimulation, glutamate, retinal prosthesis

Millions of people worldwide suffer from photoreceptor degenerative diseases, such as retinitis pigmentosa (RP) and AMD, that cause incurable visual impairment.[1,2] Triggered in many cases by genetic mutations to either the pigment epithelium or photoreceptors,[3] photoreceptor degenerative diseases result in the progressive deterioration of visual function and, eventually, death of photoreceptors, leading to a loss of vision. In addition to visual impairment, the loss of the photoreceptor layer causes a cascade of gradual remodeling in the remaining layers of the retina including the formation of rewired corrupt synapses between neurons, the development of a glial seal in the former location of the photoreceptor layer, the loss of some neurotransmitter receptors, and many other changes (see Supplementary Fig. S1).[3–5] Despite these substantial alterations and the loss of signal input from the absent photoreceptors, other retinal neurons, such as the bipolar and retinal ganglion cells (RGCs), remain intact and relatively functional in degenerated retinas.[3,5] Motivated by the presence of these remaining retinal neurons, recent research[6,7] has focused on developing therapeutic strategies to restore visual function to degenerated retinas by stimulating the surviving neurons.

Of the many therapeutic strategies being considered, the most promising thus far are electrical retinal prostheses, which use electrical current to artificially activate the surviving retinal neurons of degenerated retinas in specific patterns in the hope of restoring limited visual function to patients.[6,7] The research into electrical stimulation of the retina over the past two decades has led to the development of clinical retinal prostheses such as the Argus II and Alpha-IMS devices[7–10] that have recently been reported to provide a limited measure of visual acuity to patients, and thereby improve quality of life.[9,11] To advance retinal prosthesis-based treatment for patients, the next generation devices must be capable of restoring vision with acuity levels closer to the legal blindness limit. However, multiple studies have indicated that electrical stimulation of the retina cannot achieve substantially more spatially localized stimulation than current devices due to the electrochemical charge limit.[6,12] Furthermore, electrical current is fundamentally an unnatural means of activating retinal neurons because, unlike the neurotransmitters in normal retinas, it nonselectively

Investigative Ophthalmology & Visual Science

stimulates all types of cells in the vicinity, including passing axons, causing confusing perceptions in patients.[11–13] While some research groups continue to investigate techniques to address these limitations,[14–16] alternative therapeutic strategies like gene therapy,[17] stem cells,[18] and unconventional stimulation paradigms, such as ultrasonic,[19] photothermal,[20] or chemical stimulation[21] have been proposed to fully circumvent the limitations of electrical stimulation for restoring vision.

Of the various nonelectrical stimulation strategies proposed for activating retinal neurons, chemical stimulation is particularly promising because it offers a biomimetic means of restoring vision by stimulating retinal neurons chemically with native neurotransmitters through the same receptors used by the natural visual transduction process.[22–24] Conceptually, a microfluidics-based chemical neuromodulation strategy mimics the function of the lost photoreceptor layer with a thin microfluidic device featuring a large array of closely separated microports through which neurotransmitters are released onto surviving retinal neurons in response to patterns of light (see Supplementary Fig. S1B). The feasibility of neurotransmitter-based stimulation to generate spatially localized RGC spike rate responses similar to those evoked by visual stimulation has recently been demonstrated in wild-type (normal) rat retinas in vitro by injecting glutamate, the primary retinal neurotransmitter, at single isolated sites in both epiretinal (front of the retina) and subretinal (behind the retina) configurations.[24–26] One study has also demonstrated the feasibility of stimulating the RGCs in degenerated rat retinas in vitro by injecting glutamate at single isolated sites in the epiretinal configuration.[25] However, the feasibility of stimulating the surviving retinal neurons in degenerated retinas from the subretinal side has not been reported in the literature, although such a possibility has been suggested.[24,26,27] The subretinal application of exogenous glutamate is particularly appealing because it offers the prospect of engaging the retina's inherent visual processing circuitry as recently demonstrated in the differential stimulation of the OFF and ON pathways in wild-type rat retinas.[24] But the viability of subretinal chemical neuromodulation in degenerated retinas is not obvious because surviving retinal neurons, such as bipolar cells, are known to lose glutamate sensitivity following photoreceptor degeneration.[3,5] Furthermore, the feasibility of simultaneous multisite chemical stimulation of the degenerated retina, which is critical for accomplishing spatially patterned stimulation of the retina, has not been investigated.

In this paper, we experimentally demonstrate the feasibility of stimulating photoreceptor degenerated retinas with subretinally injected exogenous neurotransmitter glutamate using a common transgenic rat model, the S334ter-3 rat, that closely mimics the progression of photoreceptor degenerative diseases in humans.[28,29] Specifically, using a special experimental setup comprising a micropipette and a multiport microfluidic device to inject chemicals into the retina and a multielectrode array to record the spatiotemporal characteristics of the RGC responses, we show that degenerated retinas can be effectively stimulated with glutamate focally at single isolated sites as well as spatially at multiple sites. We also investigated the effects of retinal remodeling on the efficacy of chemical neuromodulation in terms of the success rate of glutamate injections at different stages of photoreceptor degeneration.

Methods

Study Design

The study design was based on controlled laboratory experiments involving in vitro stimulation of explanted photoreceptor degenerated rat retinas with the neurotransmitter glutamate using both single-port glass micropipettes and a prototype multiport microfluidic device. The objective of the study was to convectively inject pulsatile boluses of glutamate either through single micropipettes or the multiport microfluidic device into the subretinal side of photoreceptor-degenerated retinas to determine if glutamate stimulation could evoke physiologic RGC responses despite the retinal remodeling. To study chemical neuromodulation in photoreceptor degenerated retinas, we used hemizygous S334ter-3 rats bred from the homozygous S334ter-3 rat line obtained from the LaVail Laboratory[30,31] at the University of California at San Francisco. The S334ter-3 rat is a transgenic rat commonly used to model photoreceptor degeneration[23,28,29,31] as it expresses a truncated version of the murine *opsin* gene that results in a form of photoreceptor degeneration similar to the rhodopsin gene mutation found in many cases of RP in humans.[28] This specific rat model was chosen in part because of its similarity to human RP and because it exhibits relatively fast degeneration (Supplementary Fig. S2), which permitted examination of chemical neuromodulation at many different stages of photoreceptor degeneration. The S334ter-3 rat was also used because it could be easily crossbred with Long-Evans rats to produce hemizygous offspring with pigmented retinas, which are beneficial for in vitro stimulation experiments. All experiments detailed in this study exclusively used pigmented hemizygous S334ter-3 rats, as opposed to homozygous S334ter-3 rats, because the former: (1) carry only one copy of the mutant transgene, and therefore exhibit a relatively slower degeneration rate that is closer to the human condition than the latter, and (2) are more similar to pigmented wild-type Long-Evans rats that are well-studied,[32–35] and hence provide a basis for comparing the results with our previous work.

Experimental Animals

Transgenic nonpigmented homozygous S334ter-3 rats were mated with pigmented Long-Evans rats (either male or female; Charles River Laboratories, Wilmington, MA, USA) to produce pigmented hemizygous offspring expressing the S334ter transgene. To characterize glutamate stimulation in retinas exhibiting different levels of photoreceptor degeneration, a total of 20 pigmented hemizygous S334ter-3 rats of different ages based on their postnatal day (PND) were studied. Using the rates of degeneration reported by the LaVail Laboratory (Supplementary Fig. S2), these 20 rats were divided into four groups, each expressing progressively increasing levels of degeneration for experiments: early stage degeneration (14–20 PND; $N = 4$), middle stage degeneration (21–27 PND; $N = 4$), late stage degeneration (28–35 PND; $N = 6$), and completely blind (>50 PND; $N = 6$).[30,31] The use of at least four rats in each group ensured that each group contained a sufficient sample size of glutamate-responsive RGCs to permit statistical analyses of the data based on a pilot study in completely blind rats. All animal experiments were conducted in accordance with the ARVO Statement for Use of Animals in Ophthalmic and Vision Research as well as the guidelines outlined by the National Research Council's Guide for the Care and Use of Laboratory Animals. Animal handling and euthanasia protocols were reviewed and approved by the Institutional Animal Care and Use Committee of the University of Illinois at Chicago.

Sample Preparation

Following approximately 1 hour of dark adaptation, hemizygous S334ter-3 rats were euthanized using a combination of carbon dioxide and cervical dislocation. After euthanasia, the retinas were extracted from enucleated eyes and placed onto a

perforated multielectrode array (pMEA; pMEA200/30iR-Ti; Multi Channel Systems MCS GmbH, Reutlingen, Baden-Württemberg, Germany) with the ganglion cell side oriented toward the electrodes. The retina was perfused (flow rate 3 mL/min) with oxygenated (95% oxygen and 5% carbon dioxide) Ames medium (Sigma-Aldrich Corp., St. Louis, MO, USA) at room temperature (22°C). To ensure adequate perfusion, the retina was perfused from both the top through the pMEA perfusion chamber and the bottom through the perforations on the pMEA. To ensure firm contact between the pMEA electrodes and retinal tissue throughout the entire duration of the experiment, slight suction was applied to the bottom of the pMEA by removing the standard pMEA heating plate, and, consequently, all experiments were conducted at room temperature. After placing the retina on the pMEA and beginning perfusion and the bottom suction, the explanted retina was left to recover from surgical trauma for at least 30 minutes before commencing spike data recording and stimulations with glutamate. To preserve the potential light sensitivity of any remaining photoreceptors in the degenerated retinas, all sample preparation work and stimulation experiments were conducted under dim red illumination.

Experimental Setup

A specialized experimental setup (Supplementary Fig. S3) was used to enable chemical injections into the subretinal (top) side of explanted retinas while simultaneously recording the neural responses of retinal ganglion cells and visually observing the retina using an inverted optical microscope (Nikon Eclipse Ti-E; Nikon, Tokyo, Japan). The pMEA featured 60, 30-µm diameter electrodes that were located at the intersections of a square grid laid out in a (8 × 8) pattern with an interelectrode spacing of 200 µm, except the four corners. The RGC response signals picked up by the 60 electrodes of the pMEA were amplified and acquired into a computer through a pMEA system with MC_Rack software (MEA1060; Multi Channel Systems MCS GmbH). The entire pMEA system was placed over the inverted optical microscope (Nikon Eclipse Ti) to observe the retina and the chemical injections using filtered red illumination to prevent unintentional photoreceptor photobleaching. A green (570 nm) light-emitting diode (LED) was used to visually stimulate the retina with full-field flashes of light from the top and, based on its responsivity to the full-field flashes, assess the level of photoreceptor degeneration in the retina.

For single-site injections, a prepulled glass micropipette (10-µm tip diameter and 1-mm outer diameter; World Precision Instruments, Sarasota, FL, USA) was filled with glutamate solution (1 mM; Sigma-Aldrich Corp.) and inserted into a standard microelectrode/micropipette holder (QSW-A10P; Warner Instruments, Hamden, CT, USA) that was held and maneuvered over the pMEA using a three-axis, motorized, precision manipulator (MP-285; Sutter Instruments, Novato, CA, USA) with submicron positioning accuracy (Supplementary Fig. S3A). The pressure port of the micropipette holder was connected to one of the channels of an 8-channel pressure injection system (PM-8; Harvard Apparatus, Holliston, MA, USA), which was used to pneumatically eject glutamate through the micropipette tip. The micropipette tip was filled with glutamate buffered in Ames Medium (including NaCl and KCl for impedance measurements) and electrically coupled to a patch-clamp amplifier (Axopatch 200b; Molecular Devices, Sunnyvale, CA, USA) with a silver/silver chloride wire to form an electrode. Deviations in the electrode impedance from the initial impedance were used to determine contact of the micropipette tip with the retinal surface as the tip was inserted into the retina and to detect blockage of the pipette tip (e.g., occlusion with extracellular material, etc.) during an experiment.

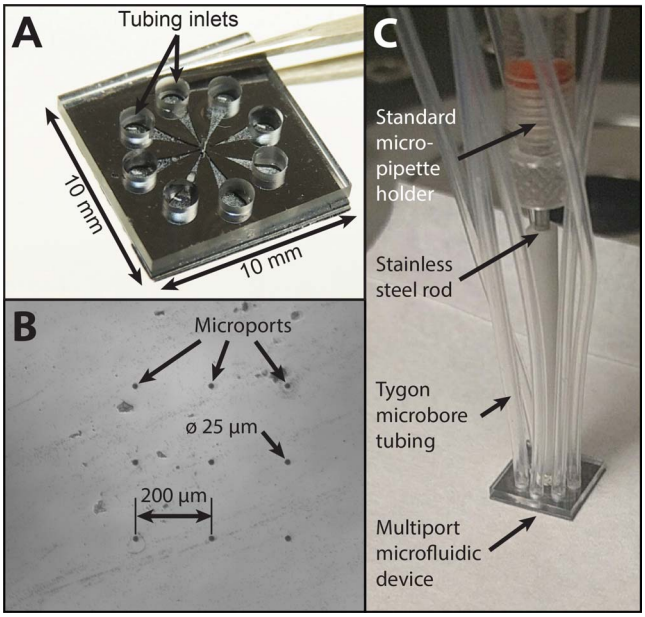

Figure 1. Prototype multiport microfluidic device. (**A**) A close-up of the multiport microfluidic device held by tweezers showing the arrangement of the eight independently addressable on-chip reservoirs and tubing inlets. (**B**) A microscope image of the bottom surface of the device showing the eight 25-µm diameter microports arranged in a 3 × 3 configuration with 200-µm spacing to align with the electrodes of the pMEA. The eight outside microports were used for multisite injections while the central microport of the 3 × 3 array was used strictly for alignment during fabrication of the device. (**C**) A photograph of the complete microfluidic device interfaced with Tygon microbore tubing connected to the pressure ports of an eight-channel pressure injector. The Tygon tubing also served as reservoirs for holding glutamate. A stainless steel rod provided a stiff support and was inserted into a standard micropipette holder.

To accomplish pattern stimulation, we fabricated a special microfluidic device comprising an array of independently addressable microports connected to tiny on-chip glutamate reservoirs via microchannels (Fig. 1A). This prototype device (1 × 1 × 0.134 cm^3), which was fabricated in two layers, consisted of eight independently addressable microports (25-µm diameter) in the bottom silicon layer (340-µm thick) and eight on-chip reservoirs (diameter 1.6 mm) for storing glutamate in the top glass layer (1-mm thick). Each of the eight microports in the bottom layer of the device was independently connected to an on-chip reservoir in the top layer via an in-plane microchannel. The eight microports were arrayed along the periphery of a 3 × 3 grid with an interport spacing of 200 µm (Fig. 1B), which corresponds to the spacing of the electrodes of the pMEA. This layout of the microports permitted the microports to be aligned over the pMEA electrodes to inject glutamate into the retina at sites directly above the electrodes, and thereby simplify the analyses of spatial spread of glutamate-responsive cells relative to the injection sites. Each of the eight on-chip reservoirs in the top layer was filled with glutamate (1 mM) and connected to a pressure port of the 8-channel pressure injection system via flexible Tygon microbore tubing (outer diameter 1.52 mm; Fig. 1C) to allow independent actuation of the microports for patterned multisite microfluidic injections. Similar to the glass micropipettes, the prototype device was held in the precision manipulator by means of a miniature stainless steel rod inserted into a standard micropipette holder (Supplementary

Fig. S3B). More details on the design and microfabrication of the prototype multiport microfluidic device can be found in Rountree et al.[36]

To achieve repeatable, high accuracy spatiotemporal modulation, synchronization of the chemical and visual stimulus events and precise positioning of the micropipette tip and prototype multiport microfluidic device over the pMEA electrodes in each experiment, all of the main instruments (pressure injector, LED, microscope, and the manipulator) in the setup were computer controlled via a digital-to-analog DAQ board (PCI-6251, 16-bit; National Instruments, Austin, TX, USA) and custom scripts coded in LabView (National Instruments).

Glutamate Stimulation

Before starting the glutamate stimulation protocol, the health of the retina sample placed on the pMEA following the surgical procedure was monitored by observing the spontaneous responses of RGCs for approximately 30 minutes. Once stabilized, the retina was investigated by injecting boluses of glutamate targeted at electrodes with robust spontaneous RGC activity. The details of glutamate stimulation using both micropipettes and the prototype multiport microfluidic device are described below.

In all experiments, L-glutamic acid was mixed with Ames Medium (1 mM; Sigma-Aldrich Corp.) and, after ensuring that the resulting pH of the mixture remained nearly unchanged ($\sim\Delta pH \leq 0.011$), loaded into either glass micropipettes or the reservoirs of the prototype multiport microfluidic device by suctioning stock glutamate solution from a Petri dish. In the single-site stimulation experiments, the micropipette tip held in the manipulator arm was positioned above target electrodes of the pMEA and lowered until contact with the retinal surface was detected[24] through an increase in the impedance of the electrode formed at the tip of the micropipette. After confirming its contact with the retinal surface, the micropipette was advanced downward to insert its tip 40-μm below the surface of the retina, which corresponds to the combined thickness of the outer nuclear layer and outer segments of the degenerated photoreceptors in the early and middle stages of degeneration,[29] to place the aperture near the remnants of the outer plexiform layer. A pilot study found that glutamate injections at this depth had the highest chance of eliciting RGC responses with large spike rate amplitudes from retinas in early through completely blind stages of degeneration despite the near complete absence of the outer nuclear layer and outer segments in the completely blind stage.[29] Small boluses of glutamate stored in the micropipette were then injected at the target location inside the retina using pressure pulses of 0.69 kPa and 30 ms triggered by the pressure injector system. Glutamate injection trials at each target location comprised three sets of 30 pulses at a constant interpulse duration of 3 seconds, where the pulse width within each set was maintained to be 10, 20, and 30 ms, respectively. Similar glutamate injection trials were repeated at multiple locations on each of the retina samples tested. Periods of spontaneous activity were recorded between injections to track the health of retinal neurons during and after glutamate stimulation.

In the subset of experiments investigating multisite stimulation, the multiport microfluidic device was maneuvered over the pMEA and the outlet microports of the device were precisely positioned above target electrodes of the pMEA. Once aligned over the target electrodes, the device was lowered until the bottom (microport side) of the device was visually confirmed (inspecting through the inverted microscope) to be in contact with the top surface of retina. Then, small boluses of glutamate stored in the on-chip reservoirs were convectively injected into the retina surface through a subset (2 or more) of the eight microports simultaneously using a pulsatile pressure (0.69–34 kPa and 30 ms pulses) triggered by the corresponding channels of the pressure injector. As in the case of the single-site stimulation experiments, each multisite stimulation experiment consisted of a series of 30 trials of injections with a 3-second interpulse duration.

Data Analysis

RGC spikes were recorded using the MC_Rack software with 10-kHz sampling (after high pass filtering with a 200-Hz cutoff) and an amplitude threshold of approximately −16 μV. After concluding each experiment, spikes from all the recordings completed during that experiment were sorted into units in MATLAB (MathWorks, Natick, MA, USA) using the wavelet clustering package, Wave_clus, developed by Quiroga et al.[37] After sorting, each unit spike train was convolved with a Gaussian kernel to calculate continuous peristimulus time histograms (PSTHs), which were then averaged across trials using custom MATLAB code. PSTHs were further analyzed by extracting the spike rate response characteristics including the spike rate amplitude and latency. The spike rate amplitude was calculated as the difference between the extrema and mean spike rate, with negative and positive amplitudes characterizing inhibitory and excitatory phases, respectively.[24] The temporal characteristics of spike rate responses were estimated by measuring the latency, which was defined as the time difference between the injection and the peak response. Responsive units were identified using a fano factor derived response variable (see Ref. 24 for details) and further filtered by excluding units with spike rates less than 3 Hz to eliminate signals uncharacteristic of typical neural responses. If responses contained more than one phase with amplitudes exceeding a spike rate threshold of 3 Hz, the largest amplitude was assumed to be the dominant response.

Individual unit spike trains were also used to calculate the interspike intervals (ISI) for each cell during both glutamate stimulation and spontaneous activity. The distribution of each unit's spontaneous and glutamate-evoked ISIs were estimated using the unit's median ISI during spontaneous and glutamate stimulation recordings. The median spontaneous and glutamate-evoked ISIs were then used for a population comparison across different stages of degeneration to observe how the introduction of exogenous glutamate affected the burst firing of RGCs in degenerated conditions.

Using the PSTH neural response data, we characterized the spatial localization of glutamate stimulation of photoreceptor degenerated retinas by determining the spatial spread of retinal responses to single-site injections with micropipettes and multisite injections with the prototype multiport microfluidic device. The spatial spreads, or distributions, of both single- and multisite glutamate stimulation experiments were investigated by mapping the locations of glutamate-responsive RGCs exhibiting somal spike shapes using the vectors separating electrodes with responsive units from the glutamate injection site(s). Somal units, as opposed to axonal units, were exclusively used in these analyses because they are nearer to glutamate receptors, the intended targets of glutamate neurotransmitter stimulation. To quantify the spatial localization, these vectors were assembled into a two-dimensional (2D) histogram via spatial binning to represent the approximate locations of electrodes where responsive RGCs were recorded. Because the electrodes of the pMEA were relatively widely spaced compared with the separation of retinal neurons, the 2D histograms were fit with a 2D Gaussian fit to provide a more continuous estimate of the spatial

localization of responsive RGCs. Similarly, the RGC responses produced by the prototype multiport microfluidic device were assembled into 2D histograms showing the locations of responsive RGCs relative to the outlet microports of the microfluidic device.

Statistical Analyses

Three classes of statistical analyses were used in this study: two-sided Wilcoxon signed-rank tests, Kruskal-Wallis with post hoc Dunn's tests, and χ^2 homogeneity tests ($\alpha = 0.05$ for all). Wilcoxon tests were used to compare the spike rate extrema of matched sample pairs drawn from spike rates recorded during glutamate injections and during spontaneous recordings as well to compare the spontaneous and glutamate-evoked median ISIs for each stage of degeneration. Kruskal-Wallis tests were used to compare retinal responses from retinas at different stages of degeneration to determine if retinal remodeling affected spike rate characteristics and, if a significant effect was observed, a post hoc Dunn's test (with Bonferroni corrections to minimize the false discovery rate) was used to perform comparisons between groups. Specifically, the Kruskal-Wallis tests were used to detect if there was a significant difference in nonmatched samples. Finally, the χ^2 homogeneity tests were used to identify significant differences in the proportions of glutamate-responsive stimuli across the stages of degeneration. Nonparametric statistical tests were chosen because all spike rate characteristics were found to be nonnormally distributed.

Results

Photoreceptor Degenerated Retinas are Responsive to Subretinal Glutamate Injections

To determine the efficacy of single-site subretinal injections of exogenous glutamate in eliciting neural responses in photoreceptor degenerated retinas at various stages of degeneration, we analyzed glutamate-evoked RGC spike data recorded from 20 retinas of S334ter-3 rats of multiple ages grouped into four stages of degeneration, namely, early stage degeneration (14–20 PND; $N = 4$), middle stage degeneration (21–27 PND; $N = 4$), late stage degeneration (28–35 PND; $N = 6$), and completely blind (>50 PND; $N = 6$) according to the degeneration rate curve reported[28,29] for the S334ter-3 rat line (see Supplementary Fig. S2). We found that exogenous glutamate (1 mM) pneumatically injected (0.69 kPa; 10- to 30-ms pulse duration) through a micropipette tip (10-μm diameter) positioned near target pMEA electrodes (Fig. 2A) at depths of approximately 40 μm below the subretinal surface (Fig. 2B) elicited robust spike rate responses that were significantly (all $P \ll 0.001$; Wilcoxon) elevated with respect to spontaneous spike rates in retinas at all four stages of degeneration. Figures 2C and 2D show two representative spike rate and raster responses to 30 trials of single-site glutamate injections from RGCs in the complete degeneration group exhibiting excitation (Fig. 2C) and inhibition (Fig. 2D). Overall, exogenous glutamate elicited significant responses in a total of 978 glutamate-responsive cells with high success rates across all degenerated groups (64%–85% in early to middle stages and 47% in completely blind; Table), comparable to or better than the success rate (~60%) previously achieved with normal retinas.[24] These data suggest that photoreceptor degenerated retinas are responsive to exogenous glutamate stimulation and the effects of retinal remodeling do not substantially reduce the efficacy of chemical neuromodulation.

Retinal Remodeling Significantly Affects Glutamate-Evoked Spike Rate Response Characteristics

Because degenerated retinas exhibit substantial anatomic and physiologic changes compared with the wild-type condition, we investigated the effects of retinal remodeling on spike rate characteristics across all four stages of degeneration by analyzing the amplitude and latency characteristics of glutamate-evoked RGC spike rate responses to single-site subsurface glutamate injections made using micropipettes. Although the interquartile ranges of the glutamate-evoked spike rate amplitudes in all degeneration stages overlapped (Fig. 3A), significant ($P \ll 0.001$; Kruskal-Wallis) differences were found among the median response amplitudes of retinas, which suggest that retinal remodeling affected the amplitudes of glutamate-evoked RGC spike rate responses. To identify the differences in glutamate-evoked responses between stages of degeneration, we performed statistical comparisons ($\alpha = 0.05$; Dunn's test) and found that the glutamate-evoked spike rate amplitudes showed a significant increase from early through middle stage degeneration followed by a significant decrease in later stages. Similarly, significant differences ($P \ll 0.001$; Kruskal-Wallis) were also observed for median response latencies (time from injection to peak response) among retinas at all stages of degeneration (Fig. 3B), presumably due to synaptic remodeling caused by photoreceptor degeneration, despite the overlapped interquartile ranges. A comparison of the latencies between different stages of degeneration revealed that glutamate-evoked spike rate responses from retinas in early and middle stage degeneration exhibit significantly ($\alpha = 0.05$; Dunn's test) faster latencies compared with retinas from the late and completely blind stages of degeneration. Combined, these data indicate that while degenerated retinas remain responsive to exogenous glutamate stimulation even in late stages of degeneration, their RGC spike rate response characteristics are significantly affected by the progression of photoreceptor degeneration.

Degeneration has Minimal Effect on Glutamate-Evoked Interspike Intervals

Previous studies have found that the loss and/or corruption of synaptic input to RGCs due to photoreceptor degeneration causes aberrant, oscillatory spike bursting[38–40] that could have a detrimental effect on visual restoration strategies.[40,41] To identify if these oscillatory spike bursts affected chemical neuromodulation, we examined how the median ISI of RGCs changed over different stages of degeneration using both spontaneous and glutamate stimulation recordings. Figure 4A shows a comparison of the median ISIs from spontaneous recordings and demonstrates that significant ($P \ll 0.001$; Kruskal-Wallis and post hoc Dunn's Test) changes to spike bursting behavior occur throughout the course of degeneration, likely caused by different oscillatory frequencies with periods ranging between 50 and 100 ms. In contrast, the median ISIs from glutamate stimulation recordings (Fig. 4B) revealed that the application of glutamate elicited consistent bursting behavior across all degeneration stages with the exception of middle stage degeneration, which exhibited significantly ($\alpha = 0.05$; Dunn's test) shorter ISIs compared with the other stages of degeneration. Notably, the glutamate-evoked ISIs were all significantly (all $P \ll 0.001$; Wilcoxon) smaller than the corresponding spontaneous ISIs at each stage of degeneration. Together, these data indicate that retinal remodeling did have a significant effect on the spontaneous spiking behavior of RGCs but did not significantly alter the

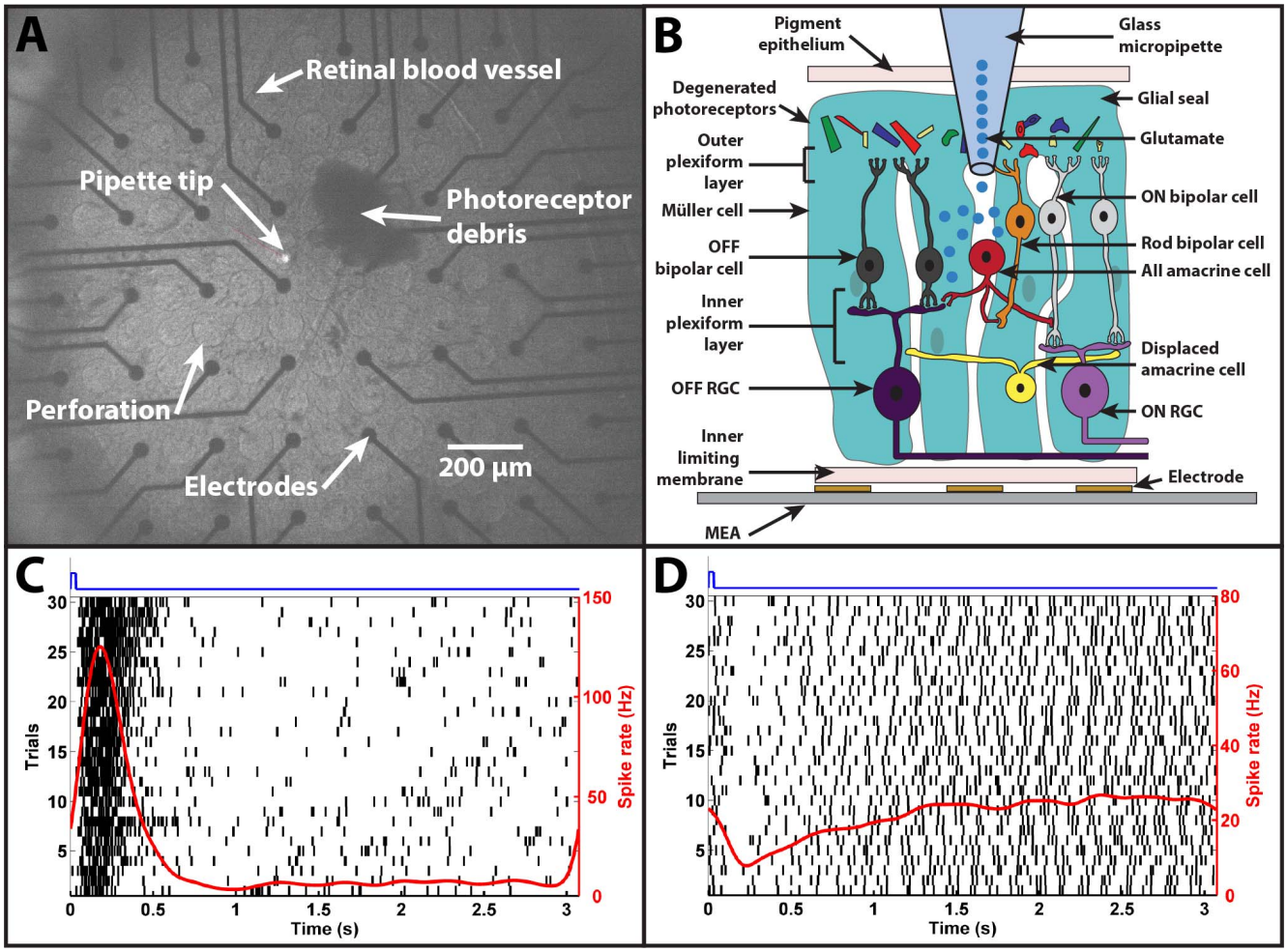

Figure 2. Subretinal glutamate injections elicit RGC responses in photoreceptor degenerated rat retinas. (**A**) An overlay image of a micropipette tip inserted into a photoreceptor degenerated retina placed over a pMEA, as viewed from the bottom of the pMEA. Boluses of 1 mM glutamate were pneumatically injected near pMEA electrodes with spiking units. (**B**) A schematic of the setup for single-site subretinal glutamate injections, which was accomplished by inserting glass micropipettes to subsurface depths of approximately 40 µm below the subretinal surface before injecting glutamate into S334ter-3 rat retinas of different ages representing different stages of photoreceptor degeneration divided into: early stage degeneration (14–20 PND), middle stage degeneration (21–27 PND), late stage degeneration (28–35 PND), and completely blind (>50 PND) groups. (**C**, **D**) Representative spike rate and raster plots from RGCs in the completely blind degeneration groups of the S334ter-3 rat model that exhibited excitatory (**C**) and inhibitory (**D**) responses to glutamate. Each plot shows a response to a 30-ms injection of glutamate (indicated by *blue trace at top*) where the *vertical black lines* in each plot represent single spikes with trials stacked vertically (*left y-axis*). The *red lines* (*right y-axis*) show the spike rate through time.

Table. Populations of RGCs in Degenerated Retinas Responsive to Subretinal Glutamate Injections and Classification of the Responses

	Responsive Units	Effective Stimuli				Significance Over Stages
Degeneration Stages	Total	Total	Excitatory	Inhibitory	Differential	Total
I. Early	290	79% (178/226)	85% (151/178)	1% (2/178)	14% (25/178)	(II, IV)
II. Middle	137	64% (141/221)	90% (127/141)	1% (1/141)	9% (13/141)	(I, III, IV)
III. Late	179	85% (121/143)	90% (109/121)	0% (0/121)	10% (12/121)	(II, IV)
IV. Blind	311	47% (181/388)	80% (145/181)	1% (1/181)	19% (35/181)	(I, II, III)

Subretinal glutamate injections elicited significant spike rate responses from RGCs (see leftmost column) in each of the 4 groups of photoreceptor degenerated retinas with differing success rates. All degenerated groups exhibited relatively high overall stimulation success rates ("Total" column) though the completely blind group was significantly ($P < 0.001$; see last column) lower than the other groups. Effective stimuli were further divided into the following groups based on the polarity of recorded spike rate responses in each stimulus: (1) exclusively excitatory responses, (2) exclusively inhibitory responses, and (3) differential stimulation (i.e., a mix of both excitatory and inhibitory responses). As can be seen, the majority of injections into degenerated retinas resulted in purely excitatory responses though a minority of inhibitory responses was present in all degenerated groups, with the highest rate found for the completely blind group. Significant differences (χ^2 homogeneity test with Bonferroni correction) between the total effective stimuli of different stages of degeneration are indicated in the far right column for early (I), middle (II), late (III), and completely blind (IV) stages of degeneration.

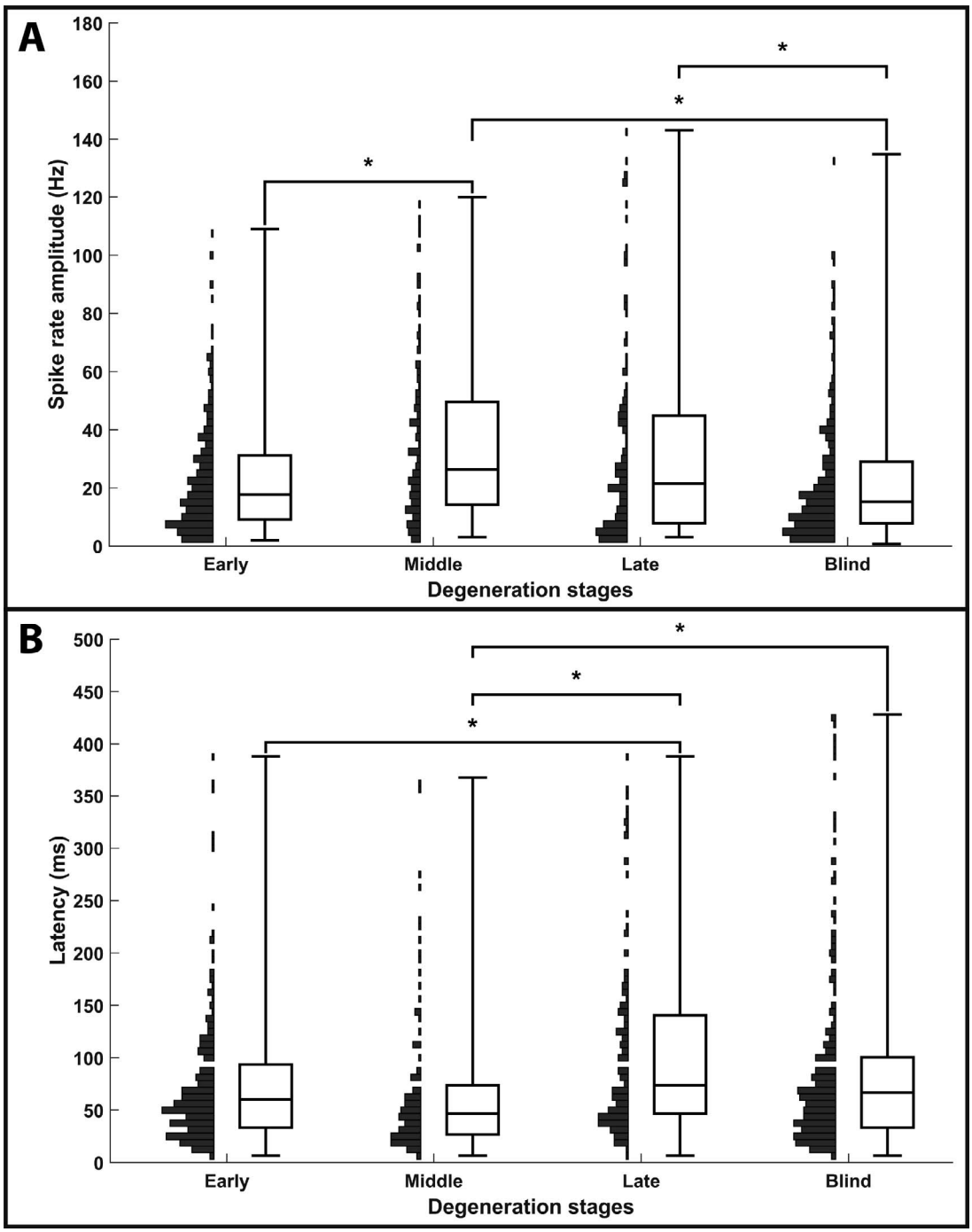

Figure 3. Amplitudes and latencies of glutamate-evoked responses exhibited by photoreceptor degenerated retinas in the four different stages of degeneration. (**A**) A comparison plot of the glutamate-evoked spike rate amplitudes recorded from RGCs in photoreceptor degenerated retinas. In each group, the lower and upper extent of the *black box* represent the lower and upper quartiles, the median is shown as a *black horizontal line*, and the maximum and minimum are shown as *whiskers* extending above and below the *box*, respectively. The distribution of data is illustrated as a histogram to the *left* of each box-and-whisker plot with 0.5-Hz bins. Photoreceptor degeneration was found to have a significant ($P \ll 0.001$; Kruskal-Wallis) effect on glutamate-evoked spike rate amplitudes. As can be seen, degeneration caused an initial significant increase in glutamate-evoked spike rate amplitudes through middle stage degeneration before dropping in the late and completely blind groups. Significant ($P < 0.05$; post hoc Dunn's test) differences between groups are shown above the box-and-whisker plots as *brackets with asterisks*. (**B**) A population level comparison plot of the latency of spike rate responses, which were found to also be significantly ($P \ll 0.001$; Kruskal-Wallis) affected by photoreceptor degeneration. The plot shows that, despite the overlapping interquartile ranges, more advanced stages of degeneration exhibited significantly ($P < 0.05$; post hoc Dunn's test) slower latencies compared with the early and middle stage groups. The distribution of latency data is shown to the left of each box-and-whisker plot as a histogram with 6.25-ms bins.

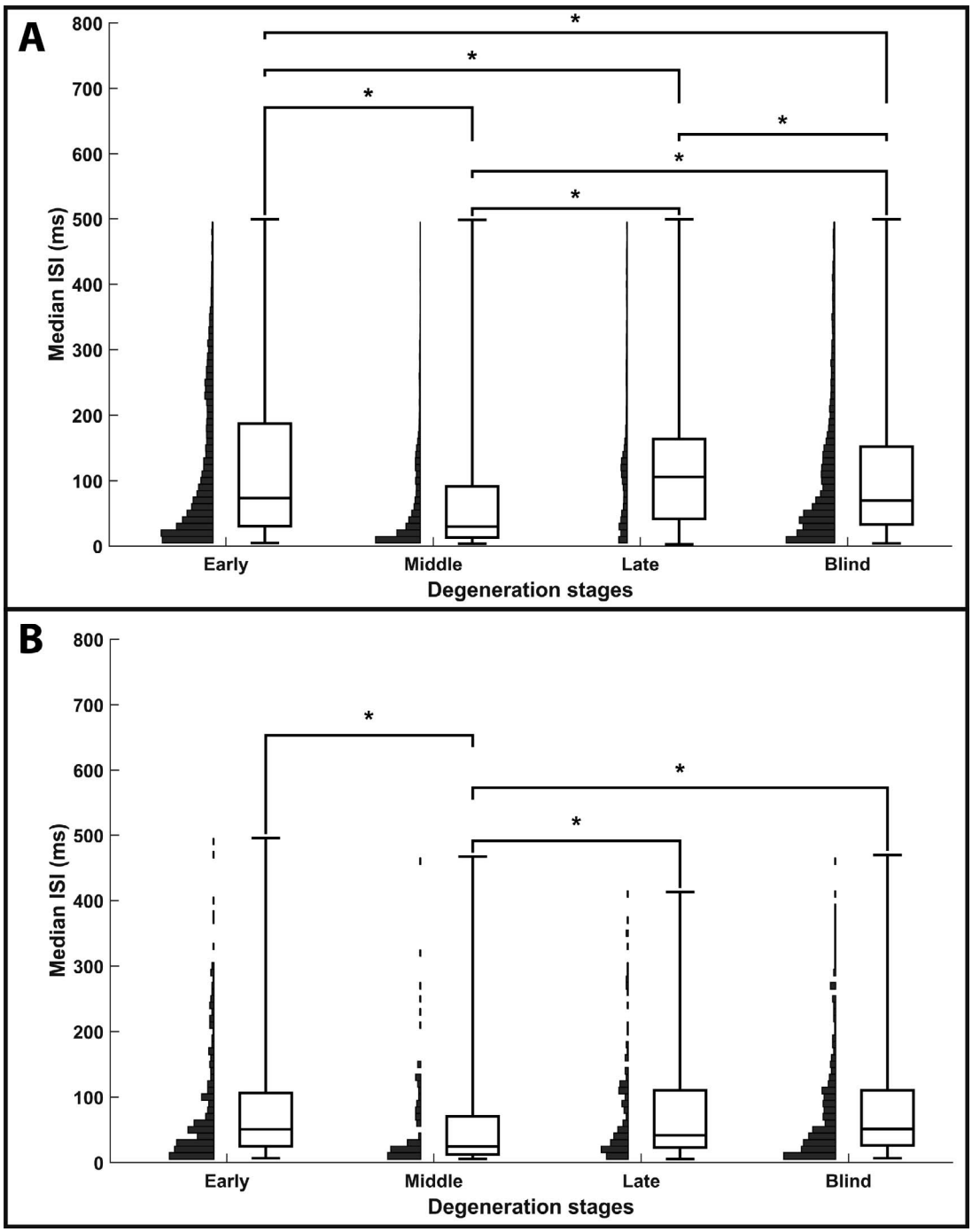

FIGURE 4. Median interspike intervals from spontaneous and glutamate stimulation recordings across different stages of degeneration. (**A**) A population level comparison plot of the median ISI during spontaneous recordings from RGCs in photoreceptor degenerated retinas. As degeneration progresses, the spontaneous ISIs display significant ($P \ll 0.001$; Kruskal Wallis with post hoc Dunn's test) differences suggesting that the spike bursting behavior of RGCs is substantially altered by the effects of retinal remodeling caused by the loss of the photorceptors. The *brackets with asterisks* above the box-and-whisker plots indicate significant differences between groups. (**B**) A similar comparison of the glutamate-evoked median ISIs shows that the application of glutamate elicited a significantly ($P \ll 0.001$; Wilcoxon) different pattern of spike bursting compared with the spontaneous condition and this pattern was consistent across all stages of degeneration except for middle stage degeneration, which had significantly ($P \ll 0.001$; Kruskal Wallis with post hoc Dunn's test) shorter ISIs. These results suggest that chemical neuromodulation can elicit consistent neural responses throughout the early, late, and completely blind stages of degeneration despite the paroxysmal spiking activity caused by retinal remodeling.

glutamate spiking behavior except during middle stage degeneration, presumably because substantial anatomic changes occur to the S334ter-3 retina during this time period.[28,42]

Exogenous Glutamate Elicits Differential Spike Rate Responses in Degenerated Retinas

To investigate whether the exogenous glutamate activated RGCs directly or indirectly through the inner nuclear layer (INL) neurons, we examined the cellular target of glutamate by analyzing the percentage of stimuli that elicited inhibitory spike rate responses (Fig. 2D). Our analyses showed that, for all glutamate stimulation in retinas at all stages of degeneration, the majority (80%–90%) elicited solely excitatory responses from RGCs while a minority (9%–19%) evoked differential (mix of both excitatory and inhibitory responses) responses (see Table). Of all stages of degeneration, completely blind retinas elicited the highest proportion of glutamate-evoked differential responses, which were significantly ($P \ll 0.001$; χ^2 homogeneity test) higher compared with earlier stages of degeneration. The presence of inhibitory responses to glutamate demonstrates indirect stimulation of RGCs through other presynaptic neurons because the ionotropic glutamate receptors expressed by RGCs, which appear to retain glutamate sensitivity throughout degeneration,[3] should result in exclusively excitatory responses. Therefore, the presence of a significant proportion of simultaneous excitatory and inhibitory responses strongly supports the hypothesis that subretinally injected exogenous glutamate can modulate RGC firing through the INL neurons, differentially stimulating the OFF and ON pathways, in photoreceptor degenerated retinas.

Glutamate Stimulation of Degenerated Retinas Evokes Spatially Localized Responses

Because achieving spatially localized stimulation is a requisite for restoring high acuity vision with any retinal prosthesis, we studied the spatial localization of glutamate stimulation and the effect of photoreceptor degeneration on localized microfluidic chemical neuromodulation by determining the spatial spread of RGCs responding to glutamate injected into the subsurface of degenerated rat retinas in all four stages of degeneration using micropipettes. The spatial spread was determined by mapping the positions of responsive somal units (see Materials and Methods) relative to the injection sites in each of the 978 sets of successful injections and plotted the resulting cumulative 2D histograms depicting the spatial distributions of glutamate responsive units in each of the four degeneration stages. Figure 5A shows a representative color map of the cumulative spatial distribution of all glutamate responsive cells from the late stage degeneration group relative to the injection site at the center of the plot, with warmer colors indicating higher densities of cells and cooler colors indicating regions with sparse responses. As can be seen, glutamate injections elicited highly localized responses (median distance of 200 μm) in retinas with late-stage degeneration. Although these spatial spread data sufficiently establish that chemical stimulations are highly localized, the relatively wide spacing of the electrodes of our pMEA likely resulted in a biased sampling of glutamate responsive units because large regions of the retina were unsampled. To obtain a more continuous estimate of the spatial distributions of glutamate responsive cells, we fit the data from the cumulative spatial distributions (such as Fig. 5A; see Supplementary Fig. S4 for the distributions of these data) for each group with a 2D Gaussian spread function (see Fig. 5B for an example for the late stage degeneration group). These spread functions fit the spatial distributions well ($r^2 > 0.98$ for all degeneration stage groups) and yielded median, upper, and lower quartiles for all four data groups (Fig. 5C). Despite the effects of retinal remodeling, chemical stimulation yielded spatially localized responses in retinas throughout all stages of degeneration with particularly low spread (i.e., high localization) in the retinas in late stage degeneration. Although the median spreads of responses of retinas across all stages of degeneration varied within a relatively small range of approximately 40 μm, we observed that spatial spread generally improved with more advanced stages of degeneration with the exception of the completely blind group. To corroborate this pattern, we examined the unfitted cumulative spatial distributions (Supplementary Fig. S4) and found that the spatial resolutions of the middle- and late-stage groups were significantly ($\alpha = 0.05$; Dunn's test) more spatially localized than the early degeneration or completely blind groups. Together, these data suggest that while photoreceptor degeneration appears to impact the spatial spread of responses to subretinal glutamate stimulation, the effects predominantly lead to small improvements in spatial localization of the stimulation.

Multisite Glutamate Stimulation of Degenerated Retinas Evokes Spatially Patterned RGC Responses

To investigate the feasibility of spatially patterned stimulation of degenerated retinas at various stages of degeneration, we stimulated the retinas at multiple sites simultaneously using a specially fabricated microfluidic device featuring an array of eight independently addressable microports connected to tiny on-chip glutamate reservoirs via microchannels. Unlike the single- site stimulations where micropipette tips were penetrated into the retinas to inject glutamate at subsurface, the microports of the microfluidic device were interfaced with degenerated retinas at the subretinal surface, where all multisite injections were delivered to spatially stimulate the retina. By independently and simultaneously activating various subsets of the eight microports using pressure pulses (10–30 ms, 0.69–34 kPa), we injected small boluses of glutamate spatially over six degenerated retinas from early (14–17 PND; $N = 4$ retinas) to middle (22–27 PND; $N = 2$ retinas) stages of photoreceptor degeneration. We found that a total of 176 RGCs responded to 41 sets of multisite glutamate injections and all responses were spatially localized around the active injection sites. Figure 6 shows the representative spatial distributions for multisite injections through two (Fig. 6B), three (Fig. 6C), and four microports (Fig. 6D) selected to resemble dot patterns of various characters. As can be seen in Figure 6, the spatial patterns of RGC responses to each multisite injection showed strong correspondence to the respective injection patterns, with the highest concentration of responsive RGCs located directly beneath active injection ports.

Discussion

This study was undertaken with three main objectives: (1) to investigate if photoreceptor degenerated retinas can be therapeutically stimulated with the neurotransmitter glutamate injected from the subretinal side, and if so, how the progression of photoreceptor degeneration affects stimulation efficacy, (2) to examine the role of inner retinal neural circuitry in the stimulation process, and (3) to explore the feasibility of achieving high spatial resolutions and eliciting patterned neural responses with glutamate stimulation in degenerated retinas. We addressed these objectives using the S334ter-3 rat as a model for human photoreceptor degenerative diseases[28,29] and a custom-built special experimental platform to inject

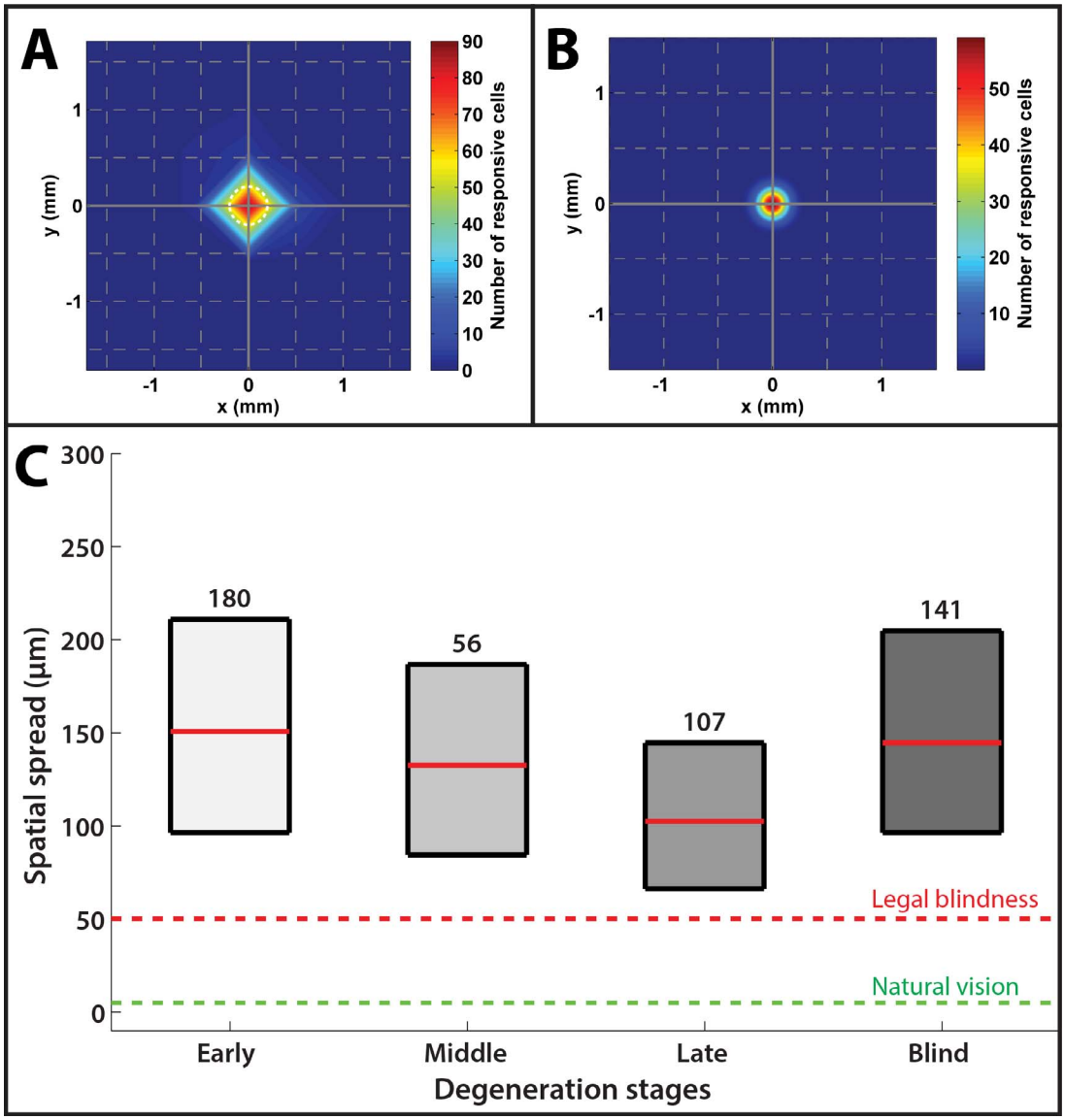

Figure 5. Spatial spread of glutamate-responsive RGCs of photoreceptor degenerated retinas in the four different stages of degeneration. (**A**) A representative 2D histogram displaying the cumulative spatial spread of responses from units with somal spike shapes (see Materials and Methods) to glutamate injections in a late stage degeneration retina, where the center is normalized to the injection site. *Warmer colors* represent higher densities of RGCs as quantified by the *color bar* on the *right*. The *gray gridlines* indicate distances of 500 µm. (**B**) Each group's spatial responses were fitted with 2D Gaussian functions to produce more continuous spatial localizations such as the one shown in plot (**B**) for the late stage degeneration group using the data from (**A**). (**C**) The lower, median (*red line*), and upper quartiles for each group derived from the 2D Gaussian models, showing that photoreceptor degeneration does not substantially reduce spatial localization. The numbers *above* each *bar* indicate the number of units with somal spike shapes in each group. The *horizontal lines* at the *bottom* of the plot indicate the retinal distances associated with the legal blindness limit (*red*) and natural vision (*green*), which correspond to standard visual acuity metrics of 1.0 and 0.0 logMAR, respectively. While subsurface injections of glutamate did not transcend the legal blindness threshold, the lower quartiles for nearly all groups were close and a minority of stimuli resulted in very localized responses below the legal blindness threshold.

chemicals into and record neural responses at multiple sites simultaneously over the retina in vitro. Our results, based on the analyses of the spatiotemporal characteristics of glutamate-evoked neural responses, demonstrate the feasibility of subretinal chemical neuromodulation of degenerated retinas. We discuss the results addressing these three objectives in the following.

Previous studies have shown that photoreceptor degeneration triggers retinal remodeling causing widespread anatomic and physiologic changes throughout the retina.[3–5] Specifically, previous studies[28,29,43–45] have found that photoreceptor degeneration generates corrupt rewired synapses that cause oscillatory, light-independent RGC spike rate patterns[38–40] that could mask or interfere with the characteristics of exogenous glutamate-evoked responses. Notwithstanding the retinal remodeling, we unexpectedly observed relatively high stimulation success rates in retinas at all stages of degeneration, although the stimulation success rate was lower in the completely blind group. Consistent with previous findings however, we found that retinal remodeling had a profound effect on the spontaneous spike rate patterns by investigating the spontaneous ISIs of RGCs, which exhibited significant differences between every stage of degeneration. Nevertheless, glutamate stimulation elicited median ISIs that were consistent

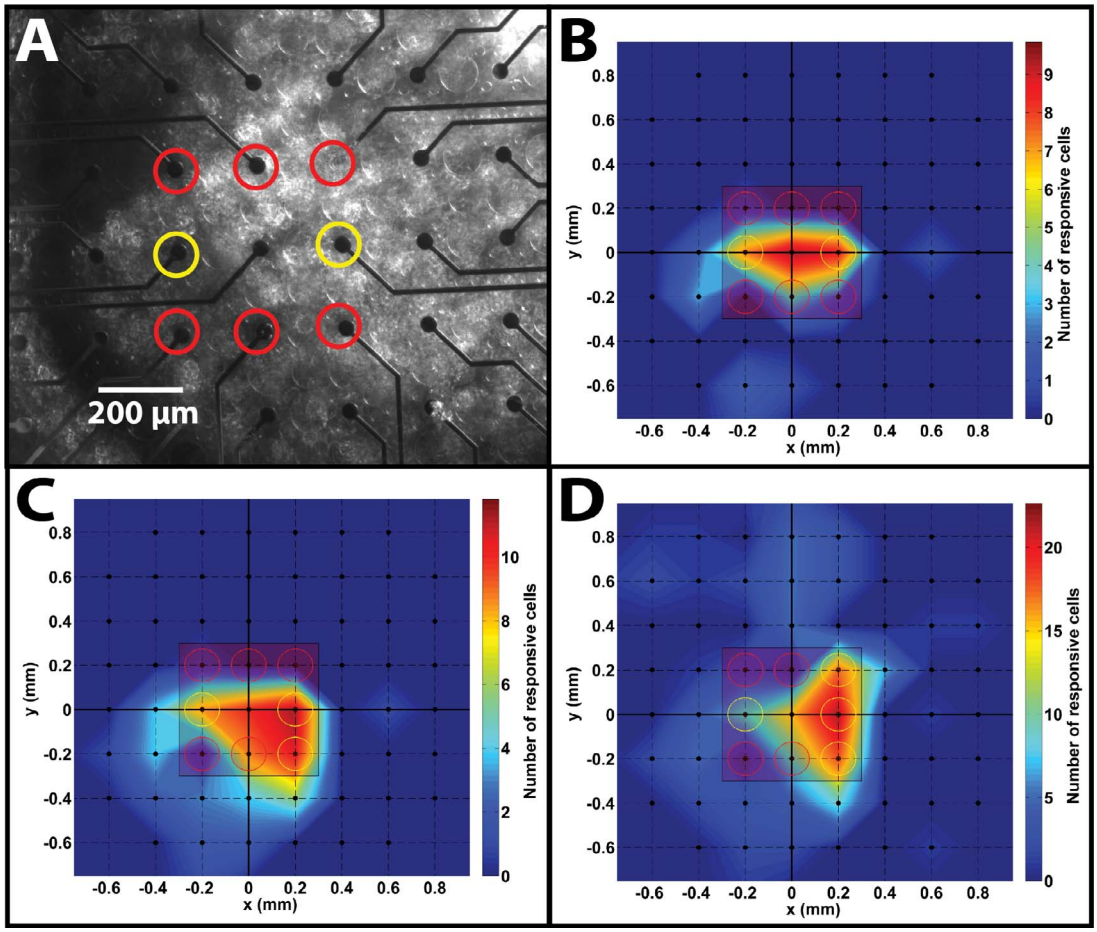

Figure 6. Multiport glutamate injections elicit corresponding RGC response patterns in degenerated retinas. An eight-port prototype multiport microfluidic device was fabricated to enable multisite surface stimulation of photoreceptor degenerated retinas. (**A**) An overlay image of a prototype chemical synapse chip interfaced with the photoreceptor degenerated retina placed over a pMEA, as viewed from the bottom of the pMEA. Prior to initiating glutamate injections, the eight microports of the chip positioned over the retina were aligned with the pMEA electrodes before pneumatically injecting glutamate through two or more active microports simultaneously (active and inactive microports are highlighted by *yellow and red circles*, respectively). (**B–D**) Plots showing 2D spatial distributions of glutamate-responsive RGCs corresponding to multisite injections using two (**B**), three (**C**), and four (**D**) microports simultaneously. Each plot shows the location of the device (*square outline*) superimposed over a color map showing the locations of all glutamate-responsive RGCs with *warmer colors* indicating higher densities of responsive cells. The black dots at the intersections of the 8 × 8 *dashed grid lines*, with the exception of the four corner intersections, represent the locations of the 60 electrodes of the pMEA. The RGC responses were spatially localized and concentrated around glutamate-injecting active microports.

across most degeneration stages and significantly different from the corresponding spontaneous ISIs. The sole exception was the middle stage degeneration group, which displayed significantly shorter ISIs in response to glutamate injections compared with other groups, consistent with the substantial anatomic changes to the S334ter-3 retina that have been reported to occur during this time period.[28,42] These results suggest that chemical neuromodulation is effective at consistently generating neural responses that overcome the abnormal, oscillatory spiking behavior observed in photoreceptor degenerated retinas.

To further explore how retinal remodeling affected the subretinal chemical stimulation, we investigated the spike rate amplitudes and temporal characteristics of RGC responses to subretinally injected exogenous glutamate in retinas at various stages of degeneration. We found that subretinal glutamate injections elicited significant RGC spike rate responses with detectable amplitudes and response latencies even in late stages of degeneration. These results show that retinal remodeling in degenerated retinas does not adversely affect the ability of exogenous glutamate in eliciting RGC responses with high signal-to-noise ratios and, unexpectedly, chemical neuromodulation yielded larger amplitudes and faster latencies compared with those reported for wild-type retinas.[24] The observed changes in amplitudes and latencies of glutamate-evoked responses in degenerated retinas compared with wild-type retinas could also have been influenced by the mere absence of the photoreceptor layer, which might have enabled a closer proximity between the injection port and target synapses.

Subretinal chemical neuromodulation of degenerated retinas would be most effective and biomimetic if RGC responses can be evoked through the surviving inner retinal circuitry by differentially stimulating the OFF and ON pathways. Such differential stimulation of degenerated retinas was not obvious or expected because photoreceptor degeneration has been previously shown to reduce or even eliminate the expression of glutamate receptors in retinal bipolar cells.[3,5] Our finding that a considerable proportion of glutamate-evoked RGC responses were driven by inhibitory inputs strongly suggests that glutamate sensitivity is preserved in at least a subset of INL neurons even in advanced stages of photoreceptor degenera-

tion because direct RGC activation with glutamate should elicit purely excitatory responses. However, the incidences of inhibitory responses in degenerated retinas (10%–20% incidence) were lower compared with similar incidence reported for the wild-type condition (~60% incidence[24]), which is probably attributable to the effects of retinal remodeling. Based on the reported literature,[3,5] the observed decline in the incidence of inhibitory responses is likely due to a combination of the loss of bipolar cell glutamate sensitivity and inner retinal rewiring, which could compromise the synaptic integrity of the ON and OFF pathways. Compared with the relatively slow progression of photoreceptor degeneration in the human condition, the rapid onset of degeneration in S334ter-3 rats[29] may have also contributed to the low incidence of inhibitory responses because the mGluR6 receptors of bipolar cells are one of the first casualties of retinal remodeling.[3] Because these remodeling effects likely stem from the lack of glutamatergic input from the lost photoreceptor layer,[3] it is conceivable that continuous, long-term subretinal glutamate stimulation in animals with slower degeneration rates more similar to the human condition could preserve the integrity of the ON and OFF pathways. Further work is needed to investigate the full potential of differential stimulation in degenerated retinas with subretinal glutamate injections, but the above results are encouraging and suggest that a measure of differential stimulation is possible even in advanced stages of photoreceptor degeneration.

We also studied the capability of subretinal glutamate injections to elicit spatially localized RGC responses, which is important for achieving high visual acuity in a prosthesis, by characterizing the spatial spreads of the responses. We found that glutamate injections into degenerated retinas resulted in spatial spreads ranging from 65 to 235 μm (lower quartile of late stage group, upper quartile of early stage group). Although the more advanced stages of photoreceptor degeneration generally exhibited more localized responses, the completely blind group displayed spatial localization comparable to early stage degeneration and the differences between any group were small (~40 μm). These data suggest that retinal remodeling has a relatively weak influence on the spatial spread of subretinal glutamate responses, and therefore, it may be feasible to achieve high visual acuities with microfluidic glutamate stimulation. If these spatial spreads observed in in vitro testing could be achieved in patients with photoreceptor degenerated retinas, they would translate to visual acuities of 1.12 to 1.63 logMAR. While these values are above the legal blindness threshold (1.0 logMAR), they represent a substantial improvement over the two current generation electrical retinal prostheses, the Argus II (restored logMARs between 1.6 and 2.9) and the Alpha-IMS (best recorded logMAR of 1.43).[10,46]

While the above studies established the feasibility of eliciting retinal neural responses at single isolated sites, multisite chemical neuromodulation of degenerated retinas, which is critical for translating pixelated patterns of visual images into neural signals in a chemical prosthesis, has never been explored before. Therefore, we explored multisite stimulation of the degenerated retina with glutamate by fabricating a special prototype multiport microfluidic device and interfacing it with degenerated retinas to inject glutamate at multiple sites simultaneously on the subretinal surface. Despite the small number (8) of relatively large size (25-μm diameter) microports in our prototype microfluidic device, we have demonstrated that it is feasible to elicit spatially localized RGC responses at multiple sites in degenerated retinas at all stages of degeneration using multiple, independently controlled injection ports. The patterns of RGC responses to multisite glutamate injections into degenerated retinas corresponded well with the arrangement of active injection ports despite the substantial physiologic and morphologic changes associated with photoreceptor degeneration, but they were relatively less spatially localized compared with the responses to glutamate injections through micropipettes. The differences in the spatial localizations in the two cases are attributable to the differences in their port geometries and interfaces with the retina. While the micropipettes featured hollow tapered needle-like ports with small diameters (10 μm) that allowed them to be positioned below the surface of the retina for injections, the multiport microfluidic device featuring larger port diameters (25 μm) was designed for surface stimulation of retinal neurons and was positioned above the retinal surface for injections. Therefore, we wondered if the presence of the glial seal near the subretinal surface would impede or even prevent surface-based stimulation using the multiport microfluidic device. However, the existence of spatially localized responses, albeit reduced compared with subsurface injections, suggests that convective glutamate injections at the subretinal surface are sufficient to penetrate the glial seal.

Chemical stimulation of retinal neurons using native neurotransmitters is a novel, biomimetic strategy that has the potential to overcome some of the limitations of current generation electrical retinal prostheses for treating photoreceptor degenerative diseases. Subretinal chemical stimulation, in particular, is more appealing because it could potentially restore more natural vision to patients by taking advantage of the retina's inherent visual processing circuitry. Our findings demonstrate that subretinal glutamate injections can successfully stimulate degenerated retinas with high spatial localization at all stages of degeneration despite the substantial anatomic and physiologic changes caused by retinal remodeling. Although further work is required to demonstrate the applicability of the chemical neuromodulation concept in in vivo animal models, the results presented in the current in vitro work offer unique insights into the challenges and opportunities of neurotransmitter-based stimulation at various stages of photoreceptor degeneration and could be used to inform the design of the next generation multiport microfluidic devices specifically optimized for in vivo testing of subretinal glutamate stimulation of photoreceptor degenerated retinas.

Acknowledgments

The authors thank Matthew LaVail, PhD, and his laboratory, at the University of California, San Francisco School of Medicine, for providing the transgenic S334ter-3 rats used for this work. They also thank Ashwin Raghunathan for his work designing, fabricating, and evaluating the multiport microfluidic device used in this study.

Supported by grants from the National Science Foundation, Emerging Frontiers in Research and Innovation (NSF-EFRI) program Grant number 0938072 (Alexandria, VA, USA).

Disclosure: **C.M. Rountree**, None; **J.B. Troy**, None; **L. Saggere**, None

References

1. Pascolini D, Mariotti SP. Global estimates of visual impairment: 2010. *Br J Ophthalmol*. 2012;96:614–618.
2. Fritsche LG, Fariss RN, Stambolian D, Abecasis GR, Curcio CA, Swaroop A. Age-related macular degeneration: genetics and biology coming together. *Annu Rev Genomics Hum Genet*. 2014;15:151–171.
3. Jones BW, Kondo M, Terasaki H, Lin Y, McCall M, Marc RE. Retinal remodeling. *Jpn J Ophthalmol*. 2012;56:289–306.
4. Jones BW, Marc RE. Retinal remodeling during retinal degeneration. *Exp Eye Res*. 2005;81:123–137.

5. Strettoi E. A survey of retinal remodeling. *Front Cell Neurosci*. 2015:494.
6. Zrenner E. Fighting blindness with microelectronics. *Sci Transl Med*. 2013;5:210ps16.
7. Humayun MS, de Juan E Jr, Dagnelie G. The bionic eye: a quarter century of retinal prosthesis research and development. *Ophthalmology*. 2016;123(10 suppl):S89–S97.
8. Humayun MS, Dorn JD, da Cruz L, et al. Interim results from the international trial of Second Sight's visual prosthesis. *Ophthalmology*. 2012;119:779–788.
9. Zrenner E, Bartz-Schmidt KU, Benav H, et al. Subretinal electronic chips allow blind patients to read letters and combine them to words. *Proc R Soc B Biol Sci*. 2011;278: 1489–1497.
10. Chuang AT, Margo CE, Greenberg PB. Retinal implants: a systematic review. *Br J Ophthalmol*. 2014;98:852–856.
11. Ahuja AK, Dorn JD, Caspi A, et al. Blind subjects implanted with the Argus II retinal prosthesis are able to improve performance in a spatial-motor task. *Br J Ophthalmol*. 2011; 95:539–543.
12. Eiber CD, Lovell NH, Suaning GJ. Attaining higher resolution visual prosthetics: a review of the factors and limitations. *J Neural Eng*. 2013;10:011002.
13. Freeman DK, Rizzo JF, Fried SI. Encoding visual information in retinal ganglion cells with prosthetic stimulation. *J Neural Eng*. 2011;8:035005.
14. Weitz AC, Nanduri D, Behrend MR, et al. Improving the spatial resolution of epiretinal implants by increasing stimulus pulse duration. *Sci Transl Med*. 2015;7:318ra203.
15. Jensen RJ, Rizzo JF III. Thresholds for activation of rabbit retinal ganglion cells with a subretinal electrode. *Exp Eye Res*. 2006;83:367–373.
16. Twyford P, Cai C, Fried S. Differential responses to high-frequency electrical stimulation in ON and OFF retinal ganglion cells. *J Neural Eng*. 2014;11:025001.
17. Boye SE, Boye SL, Lewin AS, Hauswirth WW. A comprehensive review of retinal gene therapy. *Mol Ther*. 2013;21:509–519.
18. Schwartz SD, Regillo CD, Lam BL, et al. Human embryonic stem cell-derived retinal pigment epithelium in patients with age-related macular degeneration and Stargardt's macular dystrophy: follow-up of two open-label phase 1/2 studies. *Lancet*. 2015;385:509–516.
19. Menz MD, Oralkan Ö, Khuri-Yakub PT, Baccus SA. Precise neural stimulation in the retina using focused ultrasound. *J Neurosci*. 2013;33:4550–4560.
20. Ghezzi D. Retinal prostheses: progress toward the next generation implants. *Front Neurosci*. 2015;9:290.
21. Jones PD, Stelzle M. Can nanofluidic chemical release enable fast, high resolution neurotransmitter-based neurostimulation? *Front Neurosci*. 2016;10:138.
22. Peterman MC, Mehenti NZ, Bilbao KV, et al. The Artificial Synapse Chip: a flexible retinal interface based on directed retinal cell growth and neurotransmitter stimulation. *Artif Organs*. 2003;27:975–985.
23. Iezzi R, Finlayson P, Xu Y, Katragadda R. Microfluidic neurotransmiter-based neural interfaces for retinal prosthesis. *Conf Proc IEEE Eng Med Biol Soc*. 2009;2009:4563–4565.
24. Rountree CM, Inayat S, Troy JB, Saggere L. Differential stimulation of the retina with subretinally injected exogenous neurotransmitter: a biomimetic alternative to electrical stimulation. *Sci Rep*. 2016;6:38505.
25. Finlayson PG, Iezzi R. Glutamate stimulation of retinal ganglion cells in normal and s334ter-4 rat retinas: a candidate for a neurotransmitter-based retinal prosthesis. *Invest Ophthalmol Vis Sci*. 2010;51:3619–3628.
26. Inayat S, Rountree CM, Troy JB, Saggere L. Chemical stimulation of rat retinal neurons: feasibility of an epiretinal neurotransmitter-based prosthesis. *J Neural Eng*. 2015;12: 016010.
27. Iezzi R, Finlayson PG. Neurotransmitter stimulation for retinal prosthesis: the artificial synapse chip. In: Dagnelie G, ed. *Visual Prosthetics: Physiology, Bioengineering, Rehabilitation*. New York, New York: Springer; 2011:173–190.
28. Ray A, Sun GJ, Chan L, Grzywacz NM, Weiland J, Lee E-J. Morphological alterations in retinal neurons in the S334ter-line3 transgenic rat. *Cell Tissue Res*. 2010;339:481–491.
29. Martinez-Navarrete G, Seiler MJ, Aramant RB, Fernandez-Sanchez L, Pinilla I, Cuenca N. Retinal degeneration in two lines of transgenic S334ter rats. *Exp Eye Res*. 2011;92:227–237.
30. LaVail MM. Retinal degeneration rat model resource. Available at: http://rrrc.us/userfiles/phenotyping/07021327Retinal%20Degeneration%20Rat%20Model%20Resource.pdf. Accessed December 17, 2017.
31. McGill TJ, Prusky GT, Douglas RM, et al. Discordant anatomical, electrophysiological, and visual behavioral profiles of retinal degeneration in rat models of retinal degenerative disease. *Invest Ophthalmol Vis Sci*. 2012;53: 6232–6244.
32. Young RW. The renewal of photoreceptor cell outer segments. *J Cell Biol*. 1967;33:61–72.
33. Cerro M del, Gash DM, Rao GN, Notter MF, Wiegand SJ, Gupta M. Intraocular retinal transplants. *Invest Ophthalmol Vis Sci*. 1985;26:1182–1185.
34. Zrenner E, Stett A, Weiss S, et al. Can subretinal microphotodiodes successfully replace degenerated photoreceptors? *Vision Res*. 1999;39:2555–2567.
35. Mandel Y, Goetz G, Lavinsky D, et al. Cortical responses elicited by photovoltaic subretinal prostheses exhibit similarities to visually evoked potentials. *Nat Commun*. 2013;4:1980.
36. Rountree CM, Raghunathan A, Troy JB, Saggere L. Prototype chemical synapse chip for spatially patterned neurotransmitter stimulation of the retina ex vivo. *Microsyst Nanoeng*. 2017;3:17052.
37. Quiroga RQ, Nadasdy Z, Ben-Shaul Y. Unsupervised spike detection and sorting with wavelets and superparamagnetic clustering. *Neural Comput*. 2004;16:1661–1687.
38. Soto F, Kerschensteiner D. Synaptic remodeling of neuronal circuits in early retinal degeneration. *Front Cell Neurosci*. 2015;9:395.
39. Euler T, Schubert T. Multiple independent oscillatory networks in the degenerating retina. *Front Cell Neurosci*. 2015;9: 444.
40. Trenholm S, Awatramani GB. Origins of spontaneous activity in the degenerating retina. *Front Cell Neurosci*. 2015;9:277.
41. Cho A, Ratliff C, Sampath A, Weiland J. Changes in ganglion cell physiology during retinal degeneration influence excitability by prosthetic electrodes. *J Neural Eng*. 2016;13: 025001.
42. Zhu CL, Ji Y, Lee E-J, Grzywacz NM. Spatiotemporal pattern of rod degeneration in the S334ter-line-3 rat model of retinitis pigmentosa. *Cell Tissue Res*. 2013;351:29–40.
43. Margolis DJ, Newkirk G, Euler T, Detwiler PB. Functional stability of retinal ganglion cells after degeneration-induced changes in synaptic input. *J Neurosci*. 2008;28:6526–6536.
44. Menzler J, Zeck G. Network oscillations in rod-degenerated mouse retinas. *J Neurosci*. 2011;31:2280–2291.
45. Stasheff SF, Shankar M, Andrews MP. Developmental time course distinguishes changes in spontaneous and light-evoked retinal ganglion cell activity in rd1 and rd10 mice. *J Neurophysiol*. 2011;105:3002–3009.
46. Stingl K, Bartz-Schmidt KU, Besch D, et al. Artificial vision with wirelessly powered subretinal electronic implant alpha-IMS. *Proc R Soc B Biol Sci*. 2013;280:20130077.